Journal of Magnetic Resonance 213 (2011) 69–75

Contents lists available at SciVerse ScienceDirect

Journal of Magnetic Resonance

journal homepage: www.elsevier.com/locate/jmr

Resolving overlaps in diffusion encoded spectra using band-selective pulses in a 3D BEST-DOSY experiment

Matsyendranath Shukla, Kavita Dorai *

Department of Physics, Indian Institute of Science Education & Research (IISER) Mohali, Chandigarh 160 019, India

ARTICLE INFO

Article history:
Received 14 May 2011
Revised 10 August 2011
Available online 6 September 2011

Keywords:
NMR spectroscopy
Pulsed field gradients (PFG)
Diffusion ordered spectroscopy (DOSY)
Resolution overlap
3D heteronuclear DOSY
BEST-HMQC
Carbon-13 spectroscopy

ABSTRACT

A novel diffusion-edited 3D NMR experiment that incorporates a BEST-HMQC pulse sequence in its implementation is presented. Heteronuclear 3D DOSY NMR experiments are useful in elucidating the diffusion coefficients of individual constituents of a mixture, especially in cases where the proton NMR 2D DOSY spectra show considerable overlap. The present 3D BEST-DOSY pulse sequence provides a more sensitive and less time-consuming alternative to standard 3D HMQC-DOSY experiments. Cleanly separated subspectra of individual mixture components are obtained, leading to the determination of diffusion coefficients with better accuracy. The feasibility of the technique is demonstrated on a mixture of amino acids, on a mixture of small molecules with similar diffusion coefficients, and on a complex mixture with large dynamic range (commercial gasoline). The implications of using adiabatic decoupling schemes and band-selective shaped pulses for selective BEST-DOSY experiments on proteins are also discussed.

1. Introduction

Diffusion-ordered spectroscopy (DOSY) is a powerful NMR experiment useful in separating signals from different components of a complex mixture [1–7]. Applications of the DOSY technique are plentiful and range from the analysis of polymer blends [8], residue-specific NH rates and intermolecular interactions [9,10], stacking and nanorod formation [11], molecular diffusion in cells [12], compositional analysis of block copolymers and host–guest complexes [13,14], DNA secondary structural elements [15] and mapping ligand-protein interactions [16–19]. ^{1}H DOSY spectra of molecular mixtures suffer from problems of severe signal overlap, because of the relatively narrow range of proton chemical shifts and hence a number of 3D DOSY techniques have been developed to overcome this problem, wherein additional resolution is obtained by dispersing signals in the third dimension by appending a standard 2D pulse sequence to a DOSY experiment [20–22]. Yet another route to resolve spectral overlap is to perform heteronuclear DOSY experiments using nuclei such as carbon-13 which have high chemical shift dispersion [23–26]. The experiment time is however a crucial limitation in 3D heteronuclear DOSY schemes due to the requirement of sampling in the indirect frequency dimension, with only a few increments allowed in the diffusion dimension. The overlap of spectral peaks in multi-component mixtures can severely compromise the quantitative estimation of diffusion coefficients of each component. A number of sophisticated data analysis methods have been evolved to circumvent this problem which use multi-exponential or continuous distribution fitting, which are successful only to a limited extent [27–30]. Recently, sensitivity-enhanced BEST-HMQC methods [31–33] and SOFAST-HMQC methods [34–37] were described that achieve a substantial improvement in resolution and can be used to record two-dimensional heteronuclear correlation spectra of biomolecules in very short times ranging from a few minutes to only a few seconds. The BEST type of experiments benefit from longitudinal relaxation enhancement by using shaped RF pulses while the SOFAST type of sequences have the added advantage of using Ernst-angle excitation.

This work focuses on exploiting the sensitivity-enhanced BEST-HMQC technique to achieve resolution of overlaps in a novel 3D heteronuclear ^{13}C–^{1}H diffusion ordered experiment with good sensitivity and a substantial reduction in experiment time. The method is demonstrated on a mixture of molecules with similar translational diffusion coefficients, a mixture of amino acids and a mixture of commercial gasoline. The main advantage in using a BEST-HMQC instead of the standard HMQC in a 3D DOSY scheme is the significant reduction in experimental time without a corresponding loss of sensitivity (typical 3D BEST-DOSY experiments are around four times faster than standard 3D HMQC-DOSY experiments). Several PFG sequences have been proposed to overcome problems of solvent suppression and thermal convection in proteins [38,39]. We have used band-selective pulses in the diffusion

* Corresponding author. Fax: + 91 172 2790188.
E-mail addresses: matsyendranath@iisermohali.ac.in (M. Shukla), kavita@iisermohali.ac.in (K. Dorai).

1090-7807/$ - see front matter © 2011 Elsevier Inc. All rights reserved.
doi:10.1016/j.jmr.2011.08.038

sequence in conjunction with water suppression, and implemented a selective analog of the BEST-DOSY experiment to obtain the diffusion coefficient of a model protein (lysozyme in 90% H_2O and 10% D_2O).

2. Results and discussion

The pulse sequence for the 3D BEST-DOSY experiment is given in Fig. 1. We have designed a novel fast-pulsing 3D heteronuclear diffusion experiment by concatenating a BEST-HMQC scheme with a DOSY stimulated echo based diffusion (STE) sequence. A substantial speedup in data acquisition and high sensitivity are the hallmarks of this 3D heteronuclear diffusion experiment, and are achieved by reducing the recycle delay between scans. The STE pulse sequence retains the magnetization along the z-axis during the diffusion interval, thereby minimizing losses due to fast relaxation of transverse magnetization.

The 1D ^{1}H spectra of the mixture of quinine, camphene and geraniol in methanol-d4, (Mixture 1), and the mixture of amino acids L-phenylalanine, DL-valine and L-tryptophan (Mixture 2) are shown in Fig. 2. The spectra of the mixtures show considerable overlap in resonances. The standard 2D DOSY spectra of Mixtures 1 and 2 are shown in Fig. 3, which show a set of overlapping peaks. While it is clear from the DOSY spectrum of Mixture 1 (Fig. 3a) that there are at least three components in this mixture, a closer inspection and comparison with the ^{1}H spectrum of Fig. 2a reveals overlaps between quinine and geraniol and between camphene and geraniol along the DOSY dimension, which would lead to inaccuracies in the estimation of their respective diffusion coefficients. While the solvent peak in the amino acid mixture (Fig. 3b) is separated along the diffusion dimension, none of the three amino acids could be resolved along the DOSY dimension. These overlaps could not be separated with the processing methods available with TopSpin, leading to the conclusion that a 3D extension of the DOSY method would be required to obtain accurate diffusion coefficients for each of the individual components of these mixtures.

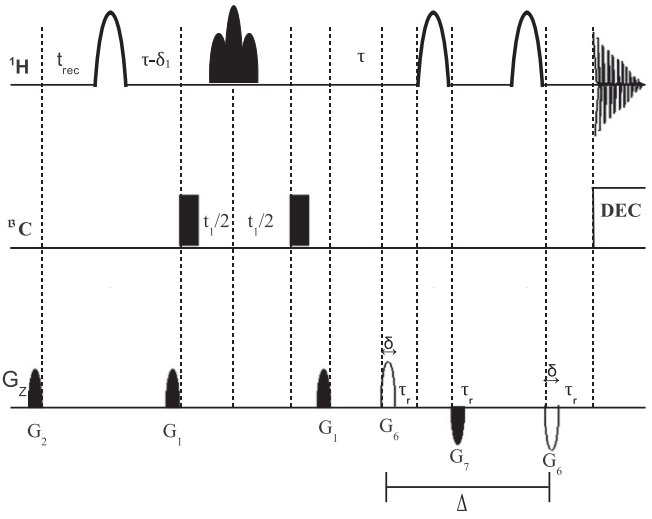

Fig. 1. Pulse sequence for the 3D BEST-DOSY experiment. τ denotes the magnetization transfer delay $1/2J_{CH}$ in the BEST-HMQC sequence and t_{rec} is the recycle delay between scans. The delay δ_1 accounts for spin evolution during the band-selective pulse and is adjusted to yield pure phase spectra in the ^{1}H dimension. The unfilled shaped pulses denote the band-selective pulses that were used for proton excitation in the desired region. Refocusing of the protons in the t_1 evolution period is achieved by the band-selective pulse denoted by the filled shape. Δ denotes the diffusion interval and the G_6 gradients are used for dephasing/rephasing magnetization during the diffusion interval. The gradient pulse lengths are denoted by δ and τ_r is the gradient recovery delay. ^{13}C decoupling during acquisition was achieved using an adiabatic decoupling sequence. For phase sensitive detection the phase of the second proton pulse is incremented according to the States-TPPI method. If no phase cycling is indicated, pulses were applied along the x-axis.

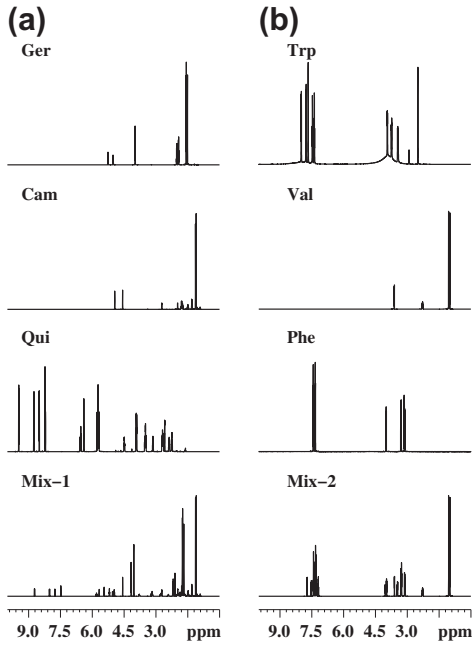

Fig. 2. The 1D ^{1}H spectra of (a) Mixture 1 with its individual components of quinine, camphene and geraniol. (b) Mixture 2 and its individual amino acid components L-phenylalanine, DL-valine and L-tryptophan. Sixteen scans were collected with 8192 complex points for each scan. Spectra were apodized with a 1 Hz exponential linebroadening function, baseline-corrected and zero-filled to minimize digitization errors. The vertical scaling factor has been adjusted so that the noise level is the same in all spectra.

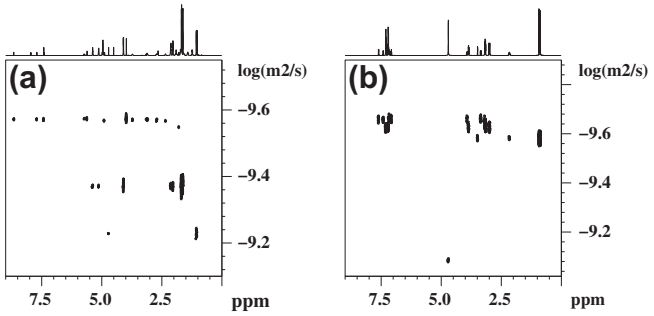

Fig. 3. 2D ^{1}H DOSY NMR spectra of (a) Mixture 1 (geraniol, camphene, and quinine) and (b) Mixture 2 (L-phenylalanine, DL-valine and L-tryptophan). Proton chemical shifts (ppm) are indicated along the x axis and diffusion units ($\log(D/m^2s^{-1})$) on the y axis.

The BEST/SOFAST-HMQC sequence is a fast-pulsing technique wherein reduced acquisition times are achieved by Ernst-angle excitation, smaller number of rf pulses and longitudinal relaxation optimization [34]. The spin states of all other unexcited protons that are not directly involved in the coherence transfer pathways remain unperturbed leading to efficiency of spin-lattice relaxation and hence reduced relaxation delays between experimental scans. The standard HMQC pulse sequence using gradients and the 2D BEST-HMQC sequence are implemented on quinine in methanol-d4 and compared in Fig. 4a and b, respectively. The ^{1}H excitation pulse is applied using a Gaussian cascade (Q5) excitation shape [40]. Band-selective ^{1}H refocusing is realized using an RSNOB pulse [41]. The pulses are centered at 3.0 ppm and cover a bandwidth of 3756 Hz and 3901 Hz corresponding to pulse lengths of 2 ms and 1.2 ms, respectively for the Q5 and RSNOB shapes at 600 MHz. The transfer delay is set to $1/(2J_{CH})$ with J_{CH} = 145 Hz. Peaks in

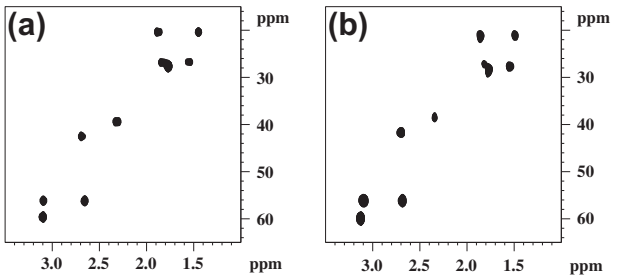

Fig. 4. Comparison of 2D $^{1}H–^{13}C$ spectra of quinine in deuterated methanol recorded at 600 MHz using (a) standard HMQC pulse sequence with gradients and (b) BEST-HMQC pulse sequence. ^{1}H excitation and refocusing covering the frequency range from 1.78 ppm to 4.0 ppm in the BEST-HMQC experiment was achieved using a Gaussian cascade (Q5) excitation [40] pulse of 2 ms and an RSNOB pulse [41] of 1.2 ms respectively. The flip angle of the excitation pulse was set at 90°. The selective pulses were centered at 3.0 ppm and had a bandwidth of 3756 Hz and 3901 Hz, respectively. The relaxation delay in the BEST-HMQC experiment was set at 200 ms and at 1 s in the HMQC experiment. ^{13}C decoupling during t_2 was realized for the standard HMQC and for the BEST-HMQC using an adiabatic decoupling sequence in both experiments.

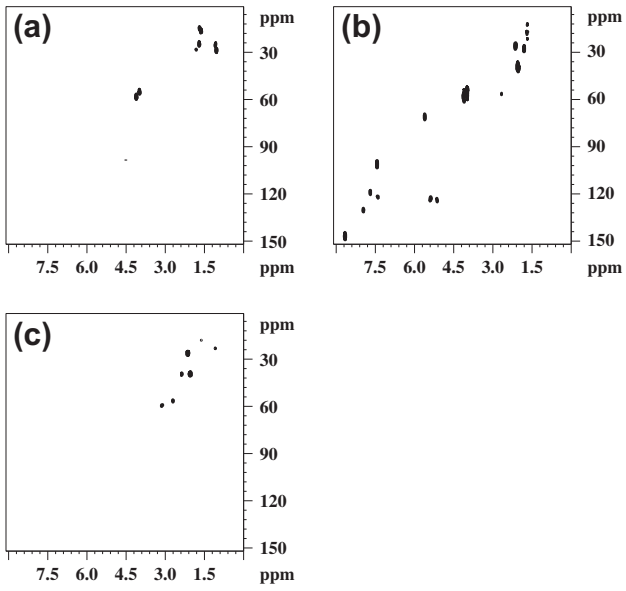

Fig. 5. BEST-HMQC planes extracted from the 3D BEST-DOSY experiment for each subspectrum in Mixture 1. BEST-HMQC subspectra of (a) geraniol, (b) quinine and (c) camphene extracted from the respective 3D experiments for diffusion coefficient ranges of $9.0 - 10.0 \times 10^{-10}$ m^2/s, $6.2 - 7.2 \times 10^{-10}$ m^2/s and $12.2 - 13.2 \times 10^{-10}$ m^2/s, respectively.

the range 1.78–4.0 ppm were excited. The S/N ratio for the peaks at 2.33 ppm/40.2 ppm, 2.68 ppm/56.2 ppm and 3.10 ppm/60.4 ppm is 59.87, 94.21 and 107.46, respectively in the standard HMQC experiment (calculated using the SINO function in Topspin). The S/N ratio for the peaks at 2.33 ppm/40.2 ppm, 2.68 ppm/56.2 ppm and 3.10 ppm/60.4 ppm is 65.98, 126.29 and 166.52, respectively in the BEST-HMQC experiment (calculated using the SINO function in Topspin). The BEST-HMQC spectrum shows a gain in signal to noise ratio as compared to the standard HMQC spectrum for quinine, all other experimental parameters including the decoupling sequence being kept the same. For both 2D experiments, 256 t_1 increments of 2K data points and 16 scans were recorded, with relaxation times of $d_1 = 1$ s and 200 ms for the standard HMQC and BEST experiments, respectively. Phase cycling followed the States-TPPI method and processing consisted of apodization using a squared cosine bell, followed by zero-filling and Fourier transformation to a 2 K × 2 K data matrix. In order to explore the efficacy of the BEST sequence in obtaining good 2D correlations we have carried out a comprehensive analysis of the Signal-to-Noise (S/N) ratios for all the three Mixtures. The data is collated in Table 1. The S/N ratios for different signals in each BEST spectrum were computed using the Topspin command SINO and compared with the S/N of the same signal in the standard HMQC experiment. The BEST experiment was repeated for three different pulse shapes: a polychromatic PC9 excitation [42], a Gaussian (Q5) wideband excitation cascade [40] and a broadband Seduce excitation shape [43]. In general we found that all three shapes gave good results. The band-selective pulses of the different shapes considered are centered at 3.0 ppm, 3.0 ppm and 4.0 ppm corresponding to a pulse length of 2.0 ms for Mixtures 1–3, respectively. Phase cycling followed the States-TPPI method and processing consisted of apodization using a squared cosine bell, followed by zero-filling and Fourier transformation to a 2 K × 2 K data matrix.

A diffusion coefficient is computed for each correlation in the 3D BEST-DOSY experiment by varying the gradient strengths in a number of experiments, concatenated into a single 3D experiment. Identical diffusion coefficients are identified as belonging to the same individual component and the BEST-HMQC correlations become "diffusion-tagged". Figs. 5 and 6 show the 2D subspectra extracted from the 3D BEST-HMQC DOSY experiments on Mixtures 1 and 2. For both experiments, three slices from the transformed 3D DOSY spectra are shown at the diffusion coefficients corresponding to the individual components. Despite spectral crowding and similarity of diffusion coefficients, the resolution in the DOSY dimension is sufficient to clearly separate the individual diffusing components. The results of the 3D heteronuclear DOSY experiments are displayed as a series of projected 2D spectra which are the integrals between given diffusion limits of the 3D spectrum with axes (ω_H,ω_C,D). At higher gradient strengths, faster diffusing components are suppressed and each spectrum is simplified. Fig. 5a–c shows projections of the BEST-HMQC subspectra from the 3D BEST-DOSY experiment on Mixture 1 corresponding to geraniol, quinine and camphene respectively onto the $\omega_H - \omega_C$ plane. The diffusion coefficients D computed from the 2D subspec-

Table 1
Comparison of S/N ratios obtained using Topspin command SINO for the standard HMQC experiment and for the BEST experiment using different shaped pulses for the three different mixtures.

Experiment	Mixture 1	Mixture 2	Mixture 3
HMQC	62.46 (2.39 ppm) 103.0 (2.67 ppm)	44.48 (2.19 ppm) 27.38 (3.05 ppm)	48.6 (1.6 ppm) 66.24 (3.21 ppm)
PC9	68.38 (2.39 ppm) 117.0 (2.67 ppm)	33.24 (2.19 ppm) 48.3 (3.05 ppm)	25.44 (1.6 ppm) 148.46 (3.21 ppm)
Q5	47.01 (2.39 ppm) 113.42 (2.67 ppm)	25.78 (2.19 ppm) 46.58 (3.05 ppm)	15.96 (1.6 ppm) 94.42 (3.21 ppm)
Seduce	103.77 (2.39 ppm) 137.1 (2.67 ppm)	36.58 (2.19 ppm) 30.27 (3.05 ppm)	22.48 (1.6 ppm) 122.04 (3.21 ppm)

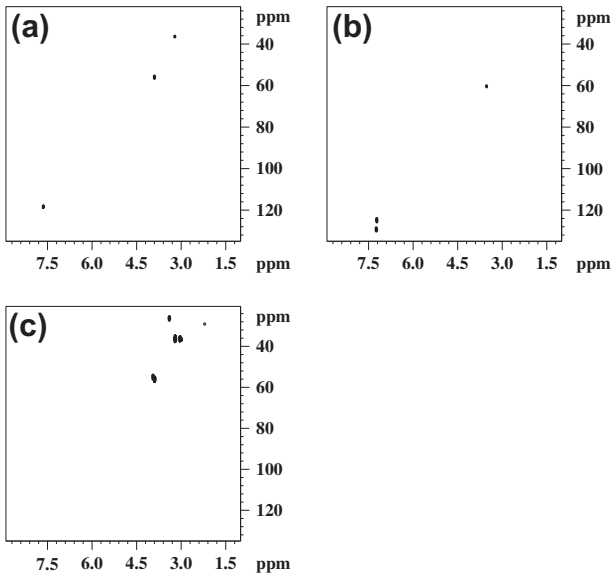

Fig. 6. BEST-HMQC planes extracted from the 3D BEST-DOSY experiment for each subspectrum in Mixture 2. BEST-HMQC subspectra of (a) L-tryptophan (b) L-phenylalanine and (c) DL-valine extracted from the respective 3D experiments for diffusion coefficient ranges of $1.5 - 2.5 \times 10^{-10}$ m^2/s, $5.0 - 6.0 \times 10^{-10}$ m^2/s and $6.0 - 7.0 \times 10^{-10}$ m^2/s, respectively.

tra turn out to be 9.0×10^{-10} m^2 s^{-1}, 6.4×10^{-10} m^2 s^{-1}, and 12.2×10^{-10} m^2 s^{-1} for geraniol, quinine and camphene, respectively. The relaxation delay was set to 200 ms and the experimental time was around 02 h. This is a substantial time savings over the previous study which performed a 3D standard HMQC-DOSY experiment on the same mixture [23] and used a total experimental time of 17 h for a total of 05 diffusion points.

Fig. 6a–c show projections of the BEST-HMQC subspectra from the 3D BEST-DOSY experiment on Mixture 2 corresponding to L-tryptophan, L-phenylalanine and DL-valine respectively. The diffusion coefficients D computed from the 2D subspectra turn out to be 1.5×10^{-10} m^2 s^{-1}, 5.2×10^{-10} m^2 s^{-1}, and 6.2×10^{-10} m^2 s^{-1} for phenylalanine, tryptophan and valine, respectively. The relaxation delay was set to 500 ms for a total experiment time of 04 h.

In both Figs. 5 and 6, almost complete resolution of the diffusion encoded spectrum is obtained with each subspectrum containing signals only from the particular individual mixture component. A good match was observed between the peaks in the 2D slice through the diffusion domain of the 3D BEST-DOSY spectrum and the 2D BEST-HMQC spectrum of the individual mixture components (spectra not shown). In order to reduce convection due to possible sample heating during the 3D experiments, a "cool" adiabatic decoupling sequence using smoothed chirp inversion pulses was used during acquisition. Using adiabatic ^{13}C decoupling enables lower powers than standard decoupling sequences such as GARP and hence less heating over a broader spectral width.

In order to demonstrate the efficacy of the BEST-DOSY technique on a "real" complex mixture, we performed the experiment on a sample of commercial gasoline. The components of gasoline can be separated into paraffins, olefins, naphthenes and aromatics and has been analyzed previously using routine ^{1}H NMR spectroscopy [44,45]. The 1D proton spectrum of gasoline is shown in Fig. 7a. The spectrum can be subdivided into aromatic (6.7–8.0 ppm), olefinic (4.6–6.0 ppm) and aliphatic (0.5–3.3 ppm) chemical shift regions. Fig. 7b shows the proton DOSY spectrum recorded on gasoline, showing considerable overlap in the diffusion coefficients. Fig. 7c–e shows projections of the BEST-HMQC subspectra from the 3D BEST-DOSY experiment on Mixture 3 corresponding to aromatics, olefins and aliphatics respectively. The diffusion coefficients D computed from the 2D BEST-HMQC subspectra for commercial gasoline turn out to be 3.3×10^{-10} m^2 s^{-1}, 5.1×10^{-10} m^{2}s^{-1}, and 8.9×10^{-10} m^{2}s^{-1} for aromatics, olefins and aliphatics, respectively. The relaxation delay was set to 200 ms for a total experiment time of 02 h. The different regions are well separated in Fig. 7 according to differences in their diffusion coefficients, indicating that the 3D BEST-DOSY experiment could be of use for high-throughput purposes and in developing quality control NMR based protocols for commercial gasoline.

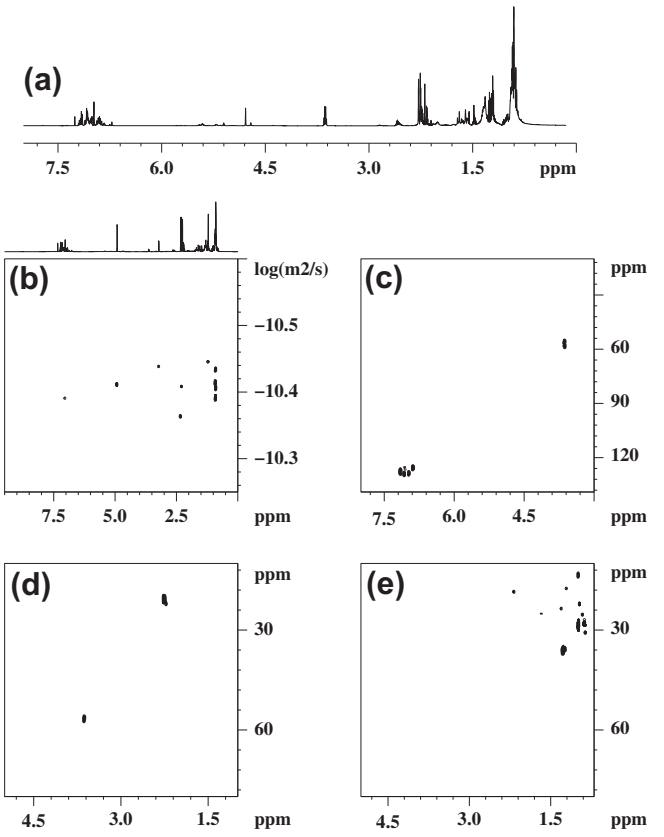

Fig. 7. (a) The 1D ^{1}H spectrum of Mixture 3 (commercial gasoline) and (b) 2D ^{1}H DOSY NMR spectrum with proton chemical shifts (ppm) indicated along the x axis and diffusion units ($\log(D/m^2s^{-1})$) on the y axis. BEST-HMQC planes extracted from the 3D BEST-DOSY experiment for each individual component in Mixture 3 of commercial gasoline are shown in (c), (d) and (e). BEST-HMQC subspectra of (c) Aromatics (d) Olefins and (e) Aliphatics extracted from the respective 3D experiments for diffusion coefficient ranges of $3.0 - 4.0 \times 10^{-10}$ m^2/s, $4.5 - 5.5 \times 10^{-10}$ m^2/s and $8.0 - 9.0 \times 10^{-10}$ m^2/s, respectively.

The average diffusion coefficients determined for the individual components of Mixtures 1–3 determined by analysis of different signals in the mixtures for the 2D DOSY and the 3D BEST-HMQC experiments are given in Table 2. The Stejskal–Tanner equation was fit to each data set using a nonlinear least squares algorithm. The second column in Table 2 has diffusion coefficient values (D in m^2 s^{-1}) measured by performing a separate 2D DOSY experiment on each individual component of both Mixtures 1 and 2. Since we did not physically separate the components of Mixture 3, the 2D DOSY experiment on each individual component was not performed on Mixture 3. The third column in Table 2 has D values computed for each individual component by extracting its 2D subspectrum from the 3D BEST-DOSY experiment. In general, there is a good agreement between the D values of components measured separately and obtained from the 3D BEST-DOSY experiment on the corresponding mixture.

Table 2
Average diffusion coefficients of the individual components of various mixtures obtained from 2D DOSY ^{1}H NMR experiments and 3D BEST-DOSY experiments.

Molecule	D (from 2D in 10^{-10} m^2 s^{-1})	D (from 3D in 10^{-10} m^2 s^{-1})
Geraniol	9.2 ± 0.5	9.0 ± 0.4
Quinine	6.6 ± 0.3	6.4 ± 0.3
Camphene	12.5 ± 0.5	12.2 ± 0.5
Tryptophan	1.7 ± 0.5	1.5 ± 0.5
Phenylalanine	5.2 ± 0.3	5.2 ± 0.3
DL-Valine	6.0 ± 0.4	6.2 ± 0.3
Gasoline (Aromatic)	–	3.3 ± 0.1
Gasoline (Olefin)	–	5.1 ± 0.1
Gasoline (Aliphatic)	–	8.9 ± 0.1

Recently a double echo PGSTE-WATERGATE sequence was developed that provides convection compensation and good solvent suppression for diffusion experiments on biomolecules [38,39]. The implementation of this pulse sequence on a small protein lysozyme (90% H_2O and 10% D_2O at a concentration of 2 mM) is shown in Fig. 8a. We have designed a selective analog of the PGSTE-WATERGATE diffusion sequence that provides good convection compensation and solvent suppression, while exciting only a desired spectral region. The 90° preparation hard pulse in the diffusion part of the pulse sequence is replaced with a band-selective Gaussian cascade (Q5) shaped pulse [40] centered at 2.5 ppm that excites resonances in the 1.0–4.0 ppm region. As seen in Fig. 8b, aliphatic proton peaks in this region are excited, with a fairly good solvent suppression. The 2D selective DOSY sequence with water suppression was concatenated with a BEST-HMQC sequence and applied on the lysozyme sample. The fit of the Stejskal–Tanner equation and the computation of the diffusion coefficient is shown in Fig. 9. The diffusion coefficient of lysozyme is determined to be $1.002 \pm 0.012 \times 10^{-10}$ m^2/s, in good agreement with previously determined values for this protein. The method offers fairly good sensitivity and would find useful application in obtaining accurate diffusion coefficients of proteins and macromolecular complexes.

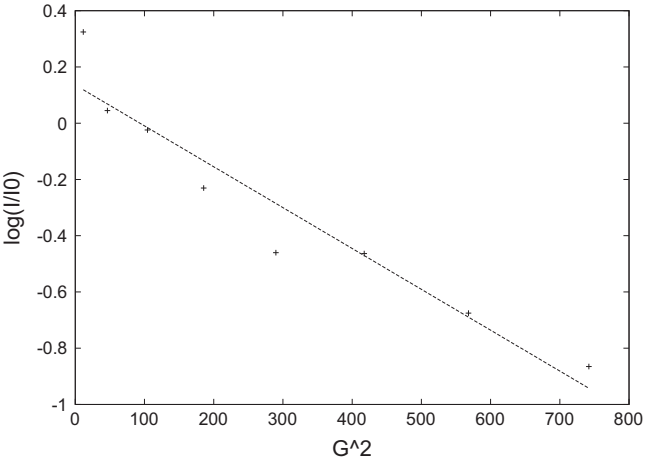

Fig. 9. The results of the BEST-DOSY experiment on lysozyme in water (10:90 D_2O/H_2O). The log of the normalized intensity is plotted with increasing gradient strength. The data were fitted to the Stejskal–Tanner equation. The diffusion coefficient is computed to be $1.002 \pm 0.012 \times 10^{-10}$ m^2/s.

3. Experimental

3.1. Model systems and spectrometer details

All the amino acids, small molecules and proteins were purchased from Sigma Aldrich and used without further purification. The NMR experiments were performed on a Bruker Avance-III 600 MHz spectrometer equipped with a 5-mm QXI probe and pulsed field gradients. TopSpin2.1 was used for recording and data processing. All diffusion experiments were performed at ambient temperature to reduce the effects of convection currents. The mixture of geraniol (20 μl), camphene (10 mg) and quinine (15 mg) in deuterated methanol is referred to as Mixture 1, the model mixture of amino acids L-Tryptophan (8 mg), DL-Valine (15 mg), and L-Phenylalanine (10 mg) in D_2O is referred to as Mixture 2 and the complex mixture of commercial gasoline (100 μl in deuterated methanol) is referred to as Mixture 3 throughout this paper.

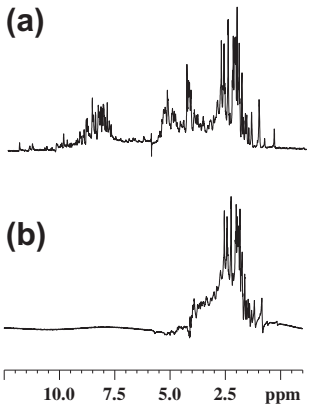

Fig. 8. 600 MHz ^{1}H spectra of protein lysozyme in water (10:90 D_2O/H_2O) acquired at ambient temperature and a low gradient strength (5%) using (a) standard WATERGATE DOSY sequence and (b) Selective DOSY sequence with water suppression and a Gaussian cascade (Q5) excitation pulse centered at 2.5 ppm. The number of scans = 32, Δ = 100 ms and δ = 4 ms. The inter-pulse delay in the binomial pulses was set to 250 μs.

3.2. 2D DOSY experiments

The signal attenuation due to action of a spin gradient echo in a DOSY pulse sequence is given by

$$S(g) = C\exp[-D(\gamma s g \delta)^2(\Delta - \delta/3)] \quad (1)$$

where D is the molecular diffusion coefficient, g is the strength of the magnetic field gradient, γ is the magnetogyric ratio, s is the shape factor of the gradient pulses (which account for the deviation of the decay due to a nonrectangular shape), Δ is the duration between the dephasing and rephasing gradient pulses and δ is the duration of the gradient pulse. The gradient pulses ranged from 1 to 3 ms in duration. The gradient field strength was varied between 2 and 34.5 G cm^{-1}. The DOSY data were obtained with a spectral window of 8000 Hz by coaddition of 32 transients for the diffusion measurements, using an acquisition time of 0.772 s and a relaxation time of 1.5 s. The FIDs were apodized by multiplication by an exponential decay function equivalent to 1-Hz line broadening and zero-filled prior to Fourier transformation to form a 8 K × 1 K

data matrix. The standard 2D DOSY processing protocol was applied in Topspin software with logarithmic scaling in the diffusion coefficient dimension. Sixteen points that make up each of the diffusion decays were fit to the Stejskal–Tanner equation using Gnuplot. Errors of the diffusion coefficient were calculated by multiplying the standard fitting error calculated within Gnuplot by the t value for the 95% confidence level.

3.3. 3D BEST-DOSY sequence

The 3D BEST-DOSY pulse sequence (Fig. 1) concatenates a BEST-HMQC experiment with a stimulated echo diffusion sequence yielding a 3D data matrix. The ^{1}H band-selective excitation pulses used for the different samples were either of a polychromatic PC9 [42], Q5 Gaussian excitation [40] or Seduce shape [43] with the excitation angle set to 90°. Band-selective ^{1}H refocusing is achieved using R-SNOB in the middle of the t_1 evolution period. The transfer delay τ is set to $1/(2J_{CH})$. The gradient ratios G_1:G_2 in the BEST sequence are set to 11:7. Δ denotes the diffusion interval and G_6 is the diffusion encoding/decoding gradient. Gradient pulse durations varied between 1.0 and 2.0 ms and The relaxation delay between scans was set to 200–500 ms. The BEST sequence excited only a selected region of protons using a band-selective pulse centered in the middle of the desired region.

The spectra were zero-filled to 8192 points in the t_3 dimension and 2048 points in the t_1 dimension. After a 2D Fourier transform using the States-TPPI method, the DOSY dimension was reconstructed on a logarithmic scale and the peaks were represented in the diffusion constant dimension on a grid of 32 data points. The HMQC subspectra were obtained by averaging slices centered at the respective diffusion coefficients. Diffusion constants were obtained by using a monoexponential fit to three resonances in each subspectrum and taking the average. Broadband adiabatic ^{13}C decoupling was achieved with a smoothed 1.5 ms chirp pulse Crp60, 0.5, 20.1 for inversion and a decoupling supercycle given in the Bruker library: P5m4sp180. The number of diffusion encoding steps in all the 3D BEST-DOSY experiments is 16, and 16 scans were recorded for a gradient pulse length δ = 2 ms and a gradient recovery time of 200 μs. Band-selective refocusing RSNOB pulse shapes [41] were used for refocusing in the BEST part of the sequence for all the mixtures. Band-selective pulses of Gaussian cascade (Q5) shape were used for Mixtures 1 and 2, respectively while band-selective pulse of Seduce shape was used for Mixture 3. Diffusion (Δ) interval times of 43 ms, 50 ms and 200 ms were used for Mixtures 1–3, respectively.

4. Conclusions

Most heteronuclear PFG NMR experiments that measure molecular self-diffusion processes face difficulties in extracting information about similar diffusion coefficients from noisy data with significant spectral overlap. While conventional 3D DOSY-HMQC experiments suffer from low sensitivity and long acquisition times for natural abundant samples, we have shown that incorporating a BEST-HMQC pulse sequence into the experiment is much less time-consuming and also has good signal-to-noise ratios. The individual NMR resonances are separated in the third dimension in the 3D BEST-DOSY experiment and monoexponential fits to peaks are used to extract diffusion coefficients. The method was demonstrated on model multi-component mixtures of amino acids small molecules and commercial gasoline. Further, a band-selective adiabatic pulse was used to construct a selective DOSY experiment with water suppression and its implementation compared with a standard WATERGATE DOSY on a protein sample. The selective DOSY pulse sequence is incorporated into a selective BEST-DOSY experiment and implemented on a small protein. An efficient and "cold" heteronuclear decoupling scheme is used which avoids problems in quantitative analysis of diffusion due to slow convection currents arising in the sample. The three components of the quinine/camphene/geraniol mixture in Mixture 1, the three amino acids in Mixture 2 and the components of commercial gasoline in Mixture 3 differ slightly in their molecular weights and hence have almost same diffusion coefficients. These model mixtures hence form a good testbed to check the accuracy of the experimental methods proposed in this work. The focus in these experiments is on reducing experiment time while retaining sensitivity and resolution overlap advantages of heteronuclear DOSY experiments. Such experiments would be useful in structure elucidation studies of mixtures, in natural product drug discovery protocols and in ligand-protein binding studies.

Acknowledgment

This work is supported by the Department of Biotechnology, Ministry of Science & Technology India, under Grant No. BT/PR9446/BRB/10/558/2007. The experiments were performed on a Bruker Avance-III 600 MHz FT-NMR spectrometer at the NMR Research Facility at IISER Mohali. MS thanks Mahamaya Singh for help in acquiring DOSY spectra and Prof Anil Kumar for useful discussions.

References

[1] W.S. Price, Pulsed field gradient nuclear magnetic resonance as a tool for studying translational diffusion: part i. Basic theory, Concepts. Magn. Reson. (1997) 299.
[2] C.S. Johnson, Diffusion ordered nuclear magnetic resonance spectroscopy:principles and applications, Prog. Nuc. Magn. Reson. 34 (1999) 203.
[3] I.K. Momot, P.W. Kuchel, Pfg nmr diffusion experiments for complex systems, Concepts. Magn. Reson. 28 (2006) 249.
[4] S. Viel, F. Ziarelli, G. Pages, C. Carrara, S. Caldarelli, Pulsed field gradient magic angle spinning nmr self-diffusion measurements, J. Magn. Reson. 190 (2008) 113.
[5] N.N. Yadav, A.M. Torres, W.S. Price, An improved approach to calibrating high magnetic field gradients for pulsed field gradient experiments, J. Magn. Reson. 194 (2008) 25.
[6] C. Carrara, S. Viel, C. Delaurent, F. Ziarelli, G. Excoffier, S. Caldarelli, Chromatographic nmr in nmr solvents, J. Magn. Reson. 194 (2008) 303.
[7] S. Caldarelli, Chromatographic nmr, Ann. Rep. NMR Spect. 73 (2011) 159.
[8] D. Li, G. Kagan, R. Hopson, P.G. Williard, Formula weight prediction by internal reference diffusion ordered nmr spectroscopy (dosy), J. Am. Chem. Soc. 131 (2009) 5627.
[9] T. Brand, E.J. Cabrita, S. Berger, Intermolecular interaction as investigated by noe and diffusion studies, Prog. Nuc. Magn. Reson. 46 (2005) 159.
[10] T. Brand, E.J. Cabrita, G.A. Morris, R. Gunther, H.J. Hofmann, S. Berger, Residue specific nh exchange rates studied by nmr diffusion experiments, J. Magn. Reson. 187 (2007).
[11] A.M. Krause-Heuer, N.J. Wheate, W.S. Price, J. Aldrich-Wright, Diffusion-based studies on the self-stacking and nanorod formation of platinum(ii) intercalators, Chem. Comm. 10 (2009) 1210.
[12] D.G. Regan, P.W. Kuchel, Simulations of molecular diffusion in lattices of cells: insights for nmr of red blood cells, Biophys. J. 83 (2002) 161.
[13] N.J. Wheate, P.G.A. Kumar, A.M. Torres, J.R. Aldrich-Wright, W.S. Price, Examination of cucurbit[7]uril and its host–guest complexes by diffusion nuclear magnetic resonance, J. Phys. Chem. B 112 (2008) 2311.
[14] S. Viel, M. Mazarin, R. Giordanengo, T.N.T. Phan, L. Charles, S. Caldarelli, D. Bertin, Improved compositional analysis of block copolymers using diffusion ordered nmr spectroscopy, Anal. Chim. Acta 654 (2009) 45.
[15] A. Ambrus, D. Yang, Diffusion-ordered nuclear magnetic resonance spectroscopy for analysis of dna secondary structural elements, Anal. Biochem. 367 (2007) 56.
[16] J. Yan, A.D. Kline, H. Mo, E.R. Zartler, M.J. Shapiro, Epitope mapping of ligand-receptor interactions by diffusion nmr, J. Am. Chem. Soc. 124 (2002) 9984.
[17] S.R. Inglis, M.J. McGann, W. Price, M.M. Harding, Diffusion nmr studies on fish antifreeze proteins and synthetic analogues, FEBS Lett. 580 (2006) 3911.
[18] W.S. Price, Protein association studied by nmr diffusometry, Curr. Opin. Coll. Inter. Sci. 11 (2006) 19.
[19] B.A. Becker, K.F. Morris, C.K. Larive, An improved method for suppressing protein background in pfg nmr experiments to determine ligand diffusion coefficients in the presence of receptor, J. Magn. Reson. 181 (2006) 327.

[20] M. Nilsson, A.M. Gil, I. Delgadillo, G.A. Morris, Improving pulse sequences for 3d diffusion ordered nmr spectroscopy: 2dj-idosy, Anal. Chem. 76 (2004) 5418.
[21] M. Nilsson, A.M. Gil, I. Delgadillo, G.A. Morris, Improving pulse sequences for 3d dosy: Cosy-idosy, Chem. Comm. 20 (2005) 1737.
[22] J.M. Newman, A. Jerschow, Improvements in complex mixture analysis by nmr: Dqf-cosy idosy, Anal. Chem. (2007) 2957.
[23] H. Barjat, G.A. Morris, A.G. Swanson, A three-dimensional dosy-hmqc experiment for the high-resolution analysis of complex mixtures, J. Magn. Reson. 131 (1998) 131.
[24] M.J. Stchedroff, A.M. Kenwright, G.A. Morris, M. Nilsson, R.K. Harris, 2d and 3d dosy methods for studying mixtures of oligomeric dimethylsiloxanes, Phys. Chem. Chem. Phys. 6 (2004) 3221.
[25] B. Vitorge, D. Jeanneat, Nmr diffusion measurements in complex mixtures using constant time hsqc-idosy and computer optimized spectral aliasing for high resolution in the carbon dimension, Anal. Chem. 78 (2006) 5601.
[26] K. Vermillion, N.P.J. Price, Stable isotope-enhanced two and three-dimensional diffusion ordered 13c nmr spectroscopy (sie-dosy 13c nmr), J. Magn. Reson. 198 (2009) 209.
[27] S.W. Provencher, Contin:a general purpose constrained regularization program for inverting noisy linear algebraic and integral equations, Comput. Phys. Commun. 27 (1982) 229.
[28] M. Delsuc, T.E. Malliavin, Maximum entropy processing of dosy nmr data, Anal. Chem. 70 (1998) 2146.
[29] B. Antalek, Using pgse nmr for chemical mixture analysis:quantitative aspects, Concepts. Magn. Reson. 30A (2007) 219.
[30] M. Nilsson, M.A. Connell, A.L. Davis, G.A. Morris, Biexponential fitting of diffusion-ordered nmr data:practicalities and limitations, Anal. Chem. 78 (2006) 3040.
[31] P. Schanda, H.V. Melckebeke, B. Brutscher, Speeding up three-dimensional protein nmr experiments to a few minutes, J. Am. Chem. Soc. 128 (2006) 9042.
[32] E. Lescop, P. Schanda, B. Brutscher, A set of best triple-resonance experiments for time-optimized protein resonance assignment, J. Magn. Reson. 187 (2007) 163.
[33] E. Lescop, T. Kern, B. Brutscher, Guidelines for the use of band-selective radiofrequency pulses in hetero-nuclear nmr: Example of longitudinal-relaxation-enhanced best-type 1h-15n correlation experiments, J. Magn. Reson. 203 (2010) 190.
[34] P. Schanda, B. Brutscher, Very fast two-dimensional nmr spectroscopy for real time investigation of dynamic events in proteins on the time scale of seconds, J. Am. Chem. Soc. 127 (2005) 8014.
[35] P. Schanda, E. Kupce, B. Brutscher, Sofast-hmqc experiments for recording two-dimensional heteronuclear correlation spectra of proteins within a few seconds, J. Bio. NMR 33 (2005) 199.
[36] P. Schanda, B. Brutscher, Hadamard frequency encoded sofast-hmqc for ultrafast two-dimensional protein nmr, J. Magn. Reson. 178 (2006) 334.
[37] T. Kern, P. Schanda, B. Brutscher, Sensitivity enhanced ipap-sofast-hmqc for fast-pulsing 2d nmr with reduced radiofrequency load, J. Magn. Reson. 190 (2008) 333.
[38] G. Zheng, T. Stait-Gardner, P.G.A. Kumar, A.M. Torres, W.S. Price, Pgste-watergate:an ste-based pgse nmr sequence with excellent solvent suppression, J. Magn. Reson. 191 (2008) 159.
[39] G. Zheng, W.S. Price, Simultaneous convection compensation and solvent suppression in biomolecular nmr diffusion experiments, J. Bio. NMR 45 (2009) 295.
[40] L. Emsley, G. Bodenhausen, Optimization of shaped selective pulses for nmr using a quaternion description of their overall propagators, J. Magn. Reson. 97 (1992) 135.
[41] E. Kupce, J. Boyd, I.D. Campbell, Short selective pulses for biochemical applications, J. Magn. Reson. 106B (1995) 300.
[42] E. Kupce, R. Freeman, Wideband excitation with polychromatic pulses, J. Magn. Reson. 108A (1994) 268.
[43] M.A. McCoy, L. Mueller, Nonresonant effects of frequency-selective pulses, J. Magn. Reson. 99 (1992) 18.
[44] G.S. Kapur, S. Berger, Simplification and assignment of proton and two-dimensional hetero-correlated nmr spectra of petroleum fractions using gradient selected editing pulse sequences, Fuel 81 (2002) 883.
[45] J. Burri, R. Crockett, R. Hany, D. Rentsch, Gasoline composition determined by ^{1}h nmr spectroscopy, Fuel 83 (2004) 187.